Segregation of chromatic and luminance signals using a novel grating stimulus

Barry B. Lee[1], Hao Sun[2] and Arne Valberg[3]

[1] *SUNY College of Optometry, New York, USA and Max-Planck Institute for Biophysical Chemistry, Göttingen, Germany*
[2] *Buskerud University College, Kongsberg, Norway and SUNY College of Optometry, New York, USA*
[3] *Norwegian University of Science and Technology, Trondheim, Norway*

Non-technical summary Signals leaving the retina must transfer information about the luminance and chromatic dimensions of the natural world. It has been suggested that, to optimize information transmission, these signals should be strictly segregated in different pathways, such as the parvocellular and magnocellular systems. Another suggestion is that signals about luminance and colour may be combined in the parvocellular pathway. We compared physiological and psychophysical responses to gratings that compound both luminance and colour to responses with pure luminance colour and gratings. The results strongly support the idea of strict segregation of luminance and chromatic signals in the afferent visual pathway.

Abstract Segregation of chromatic and luminance signals in afferent pathways are investigated with a grating stimulus containing luminance and chromatic components of different spatial frequencies. Ganglion cell recordings were obtained from the retinae of macaques (*Macaca fascicularis)*. Cell responses to the 'compound' gratings were compared to responses to standard chromatic and luminance gratings. Parvocellular (PC) pathway cell responses to compound and chromatic gratings were very similar, as were magnocellular (MC) cell responses to compound and luminance gratings. This was the case over a broad range of spatial and temporal frequencies and contrasts. In psychophysical experiments with human observers, discrimination between grating types was possible close to detection threshold. These results are consistent with chromatic and luminance structure in complex patterns being strictly localized in different afferent pathways. This novel stimulus may prove useful in identifying afferent inputs to cortical neurons.

(Received 19 February 2010; accepted after revision 4 October 2010; first published online 11 October 2010)
Corresponding author B. B. Lee: SUNY Optometry, 33 W. 42nd St, New York, NY 10036, USA. Email: blee@sunyopt.edu

Abbreviations cpd, cycles deg^{-1}; MC, magnocellular; PC, parvocellular.

DOI: 10.1113/jphysiol.2010.188862

The Journal of Physiology

Introduction

Studies of primate vision often use either luminance or chromatic modulation in an attempt to isolate postreceptoral mechanisms. There is good evidence for separable psychophysical channels for detection of luminance or chromatic changes; detection of the latter can be mediated by either red–green (long (L) and middle (M) wavelength cone opponent) or blue–yellow (short (S) wavelength cone) opponent mechanisms (Kelly & van Norren, 1977; Stromeyer *et al.* 1987; Cole *et al.* 1990; Smith *et al.* 1995). There is substantial evidence that the physiological substrates of these channels lie in the magnocellular (MC), parvocellular (PC) and koniocellular (KC) pathways, respectively (Lee *et al.* 1990, 1993*a*). Also, the MC pathway forms a substrate for a luminance channel responsible for heterochromatic flicker photometry and other photometric tasks (Lee *et al.* 1988; Kaiser *et al.* 1990; Valberg *et al.* 1992).

The role of these systems in spatial vision is more uncertain. The high contrast sensitivity of MC cells may give them an advantage in spatial vision tasks. The MC pathway appears to be primarily responsible for performance in the hyperacuities (Lee *et al.* 1993*b*, 1995; Rüttiger *et al.* 2002), for which spectral sensitivity conforms to the luminosity function (Rüttiger & Lee, 2000; Sun *et al.* 2003), as does grating acuity (Pokorny *et al.* 1968). The luminosity function is usually a signature of MC cell activity.

Natural scenes usually contain both chromatic and luminance components. There are two current hypotheses as to the neural coding of such patterns. It has been proposed that transmission of information through the optic nerve is optimized by strict segregation of luminance and chromatic information in separate channels (Buchsbaum & Gottschalk, 1983; van der Twer & MacLeod, 2001), corresponding to additive or subtractive combinations of cone signals. The high degree of correlation of M- and L-cone signals means that a segregation of this sort optimizes information transmission in a system of limited bandwidth, where noise in ganglion cell signals limits transmission (MacLeod & van der Twer, 2003). The contrary hypothesis suggests that both luminance and red–green chromatic information can be multiplexed within the PC pathway (Ingling & Martinez-Uriegas, 1983; Lennie & D'Zmura, 1988). By combination of chromatic signals, an achromatic signal might be extracted at a cortical level. This hypothesis has seldom been subject to stringent experimental testing, although Valberg *et al.* (1992) found that it was difficult to generate a suitable luminance signal for the minimal distinct border task by combining PC cell signals.

In most studies using gratings with both luminance and chromatic contrast, both have the same spatial frequency. However, there are gratings for which this is not the case, and an example is shown in Fig. 1. Alternate red and green equiluminant bars are separated by dark bars. The luminance component of the stimulus has twice the spatial frequency of the chromatic component, and if the grating is drifted, it has twice the temporal frequency as well. Chromatic and luminance gratings are shown for comparison.

We have carried out physiological and psychophysical experiments with this stimulus, which we call a compound grating. We measured macaque retinal ganglion cell spatial contrast response functions using compound, luminance and chromatic gratings and compared MC and PC cell responses. We also measured human psychophysical spatial contrast detection and discrimination functions for the three grating types; similar experiments were performed with gratings targeted at the S-cone pathway. The results support a segregation of luminance and chromatic information in the MC and PC pathways, respectively, and argue against a multiplexing model, even at high spatial frequencies. Lastly, MC and PC cell responses have distinctive signatures to compound gratings that may prove useful for identifying MC and PC contributions to, for example, the electroretinogram (Parry *et al.* 2010) or input to cortical neurons (Chen *et al.* 2007).

Methods

Physiology

Apparatus and stimuli. Visual stimuli were generated via a VSG series 2/3 graphic controller (Cambridge Research Systems, Rochester, UK) and presented on a CRT monitor (SONY Trinitron GDM-F500, 150 Hz frame rate) 2.28 m away from the monkey. Stimuli were horizontal gratings of the following types presented in a 5 deg × 5 deg window: (1) a compound red–green grating (see below for a description of stimulus structure), (2) an equiluminant red–green grating, (3) a luminance grating, all of the same mean luminance and chromaticity. The three types of gratings were drifted downwards, with the luminance grating drifted at twice the temporal frequency of the others (so that frequency was matched to the luminance component of the compound grating). For each cell, a range of spatial and temporal frequencies and contrasts was investigated. We also designed a set of gratings aimed at the S-cone ganglion cells, i.e. compound tritan (with both luminance and S-cone modulation), tritan (with S-cone modulation only) and luminance gratings. Similarly, these sets of gratings also had the same mean luminance and chromaticity. A detailed description of stimulus generation and definition of chromatic contrast is given in the Appendix.

The spectrum of each phosphor was measured using a PhotoResearch Spectroradiometer. The chromaticity

and relative luminance (10 deg $V(\lambda)$) of each phosphor was calculated by multiplying each spectrum with cone fundamentals (Smith & Pokorny, 1975) modified to the CIE 1964 10 deg colour matching and luminosity functions (Shapiro *et al.* 1996). For measurements of PC and MC cell responses, the mean luminances of the red and green phosphors were set equal to give a mean luminance of 31.34 cd m^{-2} with a chromaticity of (0.436, 0.476) in CIE x, y coordinates. Each phosphor was then modulated as described in eqns (2) and (3). For measurements of cells with S-cone input, phosphor levels required for S-cone-isolating equiluminant stimulation (i.e. tritan) were calculated and these values then also used for the luminance and compound conditions, using appropriate modifications of eqns (2) and (3). Mean luminance was 26.11 cd m^{-2} and chromaticity (x, y: 0.200, 0.161).

Procedures. All procedures strictly conformed to the National Institutes of Health *Guide for the Care and Use of Laboratory Animals* and were approved by the SUNY State College of Optometry Animal Care and Use Committee. Our experiments are consistent with the policies and regulations of *The Journal of Physiology* (Drummond, 2009). Macaques (4 male *M. fascicularis*, 2.2–3.8 kg; when cellular recordings were stable, further data were obtained with other experimental protocols) were initially sedated with an intramuscular injection of ketamine (10 mg kg^{-1}). Anaesthesia was induced with sodium thiopental (10 mg kg^{-1}) and maintained with inhaled isoflurane (0.2–2%) in a 70:30 N_2O–O_2 mixture. Local anaesthetic was applied to points of surgical intervention. EEG and ECG were monitored continuously to ensure animal health and adequate depth of anaesthesia. Muscle relaxation was maintained by an infusion of gallamine triethiodide (5 mg kg^{-1} h^{-1} I.V.) with accompanying dextrose Ringer solution (5 ml kg^{-1} h^{-1}). Careful monitoring of the EEG (and ECG) was carried out during recording and any increase in heart rate or indication from the EEG of inadequate anaesthesia was controlled by an increase in the isoflurane level. Body temperature was kept close to 37.5°C. End-tidal CO_2 was kept close to 4% by adjusting the rate and depth of respiration. At the termination of recording, the animals were killed with an overdose of sodium pentobarbital (120 mg kg^{-1}).

Neuronal activity was recorded directly from retinal ganglion cells by an electrode inserted through a cannula entering the eye behind the limbus. The details of the preparation can be found elsewhere (Crook *et al.* 1988). A gas-permeable contact lens of the appropriate power was used to bring stimuli into focus on the retina. We recorded responses of cells between 4 deg and 12 deg eccentricity. Cell identification was achieved through standard tests (Lee *et al.* 1989*b*). These included achromatic contrast sensitivity and responses to lights of different chromaticity. Additional tests, e.g. measuring responses to heterochromatically modulated lights (Smith *et al.* 1992), were employed in cases when identification was difficult. PC cells can generally be identified by their tonic responses and spectral opponency, and MC cells by their phasic responses and lack of spectral opponency. For each cell, the locus of the receptive field centre was determined and the stimulus was centred on this point. Times of spike occurrence were recorded to an accuracy of 0.1 ms, and averaged histograms of spike trains were simultaneously accumulated with 64 bins per cycle of modulation.

Psychophysics

Apparatus and stimuli. Similar apparatus and stimuli were used in psychophysical experiments. Visual stimuli were generated via either a VSG graphic controller (Series 2/5, Cambridge Research Systems, Rochester, UK) and presented on a CRT monitor (Trinitron GDM-F500, 150 Hz frame rate) or a VSG series 2/3 graphic controller (Cambridge Research Systems) and presented on a LG CRT monitor (LGFlatron 915FTPlus, 100 Hz frame rate).

The three types of grating stimulus (compound, equiluminant and luminance grating) were presented in a circular window and were drifted downwards at 0.5 Hz for the compound and equiluminant gratings, and at 1 Hz for the luminance grating so that the temporal frequency of the luminance component was matched between the luminance and the compound gratings. The spatial frequency of the gratings was varied from 0.1 to 22.0 cycles deg^{-1} (cpd) either by changing the stimulus spatial frequency on the monitor or by increasing viewing distance. The viewing distance for 0.1–1.5 cpd gratings was 0.48 m. It was increased to 3.6 m for 1.5–6 cpd gratings; and to 7.2 m for 6–22.0 cpd gratings. The stimulus size (i.e. the circular window size) was 25 deg at 0.48 m, 3.5 deg at 3.6 m and 1.7 deg at 7.2 m. Some frequencies were tested at both 0.48 m and 3.6 m, and some at both 3.6 m and 7.2 m; this was done to check that reducing stimulus size had minimal effect on the performance. The mean luminances and chromaticities of the grating stimuli were the same as those in the physiological experiment, except the isoluminant match between red and green guns were set by each individual observer using a method of minimal motion. The mean luminance of the three types of gratings were the same, 24.36 cd m^{-2}, and the mean chromaticities of the gratings were (0.439, 0.475) in CIE (x, y) coordinates, which appears yellowish to observers with normal colour vision. Surround chromaticity was the same as the target, and the luminance was fixed at 10% of that of the stimulus.

Observers. Four observers participated in the experiments. Observer H.S. was among the authors, and observers D.W., J.F. and Z.L. were naive observers who provided informed written consent according to a protocol conforming to the *Declaration of Helsinki* and Association for Research in Vision Ophthalmology. The experimental procedures were approved by the Institutional Review Board of the SUNY College of Optometry.

All observers have normal colour vision as assessed with Ishihara pseudoisochromatic plates and the Farnsworth-Munsell 100-Hue Test. Observers H.S., D.W. and Z.L. are myopic and wore contact lenses during experiments. Observer D.W.'s data were obtained with the VSG 2/5 graphic controller and the SONY CRT monitor; the other observers' data were collected with the VSG 2/3 graphic controller and the LG Electronics CRT monitor.

Procedures. We measured grating detection thresholds with a 2-down-1-up staircase method in a temporal 2-alternative-forced-choice procedure. The observer pressed a button to start the experiment. During each trial, the observer was shown two presentations, each of which was indicated with a beep. The stimulus was presented randomly in one of the two presentations, and the other one was blank. The observer's task was to indicate which presentation contained the stimulus. The visual target was viewed foveally and monocularly with the aid of a fixation cross. Each staircase was terminated after 12 reversals, and the threshold was calculated as the average of last 6 reversals.

We measured discrimination thresholds between compound and luminance gratings, and also between compound and chromatic gratings using similar staircase methods. For these measurements, in the two presentations one contained a compound grating and the other contained a luminance (or chromatic) grating, and the observer's task was to indicate which stimulus contained a chromatic (for discrimination between compound and luminance gratings) or luminance (for discrimination between compound and chromatic gratings) component.

Results

Prediction of cell responses

The compound grating is generated by alternated raised cosine waveforms from the red and green guns of the monitor (see Appendix). It thus includes both luminance and chromatic modulation. Figure 2*A* shows a compound stimulus waveform together with waveforms for luminance and chromatic gratings; all have the same mean luminance and chromaticity. The doubling of spatial frequency for the luminance component of the compound grating relative to the chromatic component is apparent. To visualize such a grating, the waveforms of the red and green components of the compound grating can be compared to the actual grating sketched in Fig. 1. There is a large family of gratings with the same luminance profile but chromatic components of different spatial frequencies and phases. That chosen had a high chromatic contrast, as defined in the Appendix.

We calculated the L- and M-cone excitations for the three gratings (Fig. 2*B*) based on the chromaticities of the display phosphors. For purposes of comparison in this and subsequent figures, we show two cycles of the luminance grating but only one cycle of the chromatic and compound gratings, so that the luminance (between compound and luminance gratings) and the chromatic (between compound and chromatic gratings) spatial frequencies and cycles are matched.

From L+M and L–M signals, we predicted the MC and PC cell responses to such gratings based on a linear model. We assumed a standard difference-of-Gaussians receptive field model, and took receptive field parameters from the literature. The upper receptive field profiles in Fig. 2*C* represent a red on-centre and a green on-centre PC cell with a centre/surround weighting of 1.15 (Derrington *et al.* 1984; Lee *et al.* 1987), and a ratio of surround to centre radius of 3:1 (Croner & Kaplan, 1995; Lee *et al.* 1998). Cone-specific inputs to centre and surround were assumed, although mixed input to the surround did not significantly affect the model responses. For the MC cell, the centre radius is 1.5 times larger than for the PC cell with a centre/surround weighting of 3:1 (Derrington & Lennie, 1984). Both M and L cones were assumed to provide input to centre and surround.

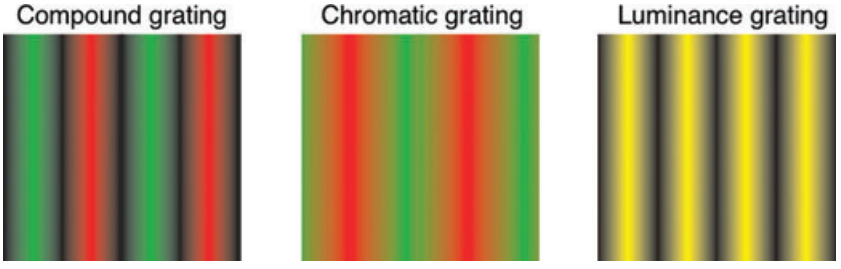

Figure 1. A novel grating stimulus
In the compound grating, coloured bars (in this case red and green) are separated by dark regions. Chromatic and luminance gratings of matched spatial frequencies are shown for comparison.

Figure 2*D* shows the responses of model cells for a close-to-optimal spatial frequency. The PC cell models respond primarily to the chromatic component, with a vigorous response to the chromatic and compound grating and a less vigorous response to the luminance grating, as expected from the opponency and low achromatic contrast sensitivity of this cell type. To the compound grating, there is only one response peak with some higher harmonic distortion. Actual responses will be rectified since firing rates cannot be negative, and the shaded areas indicate those regions of the response structure that are expected to be lost. The MC cell model responds to the luminance component of the gratings, with a vigorous response to the luminance and compound gratings and little response to the chromatic grating.

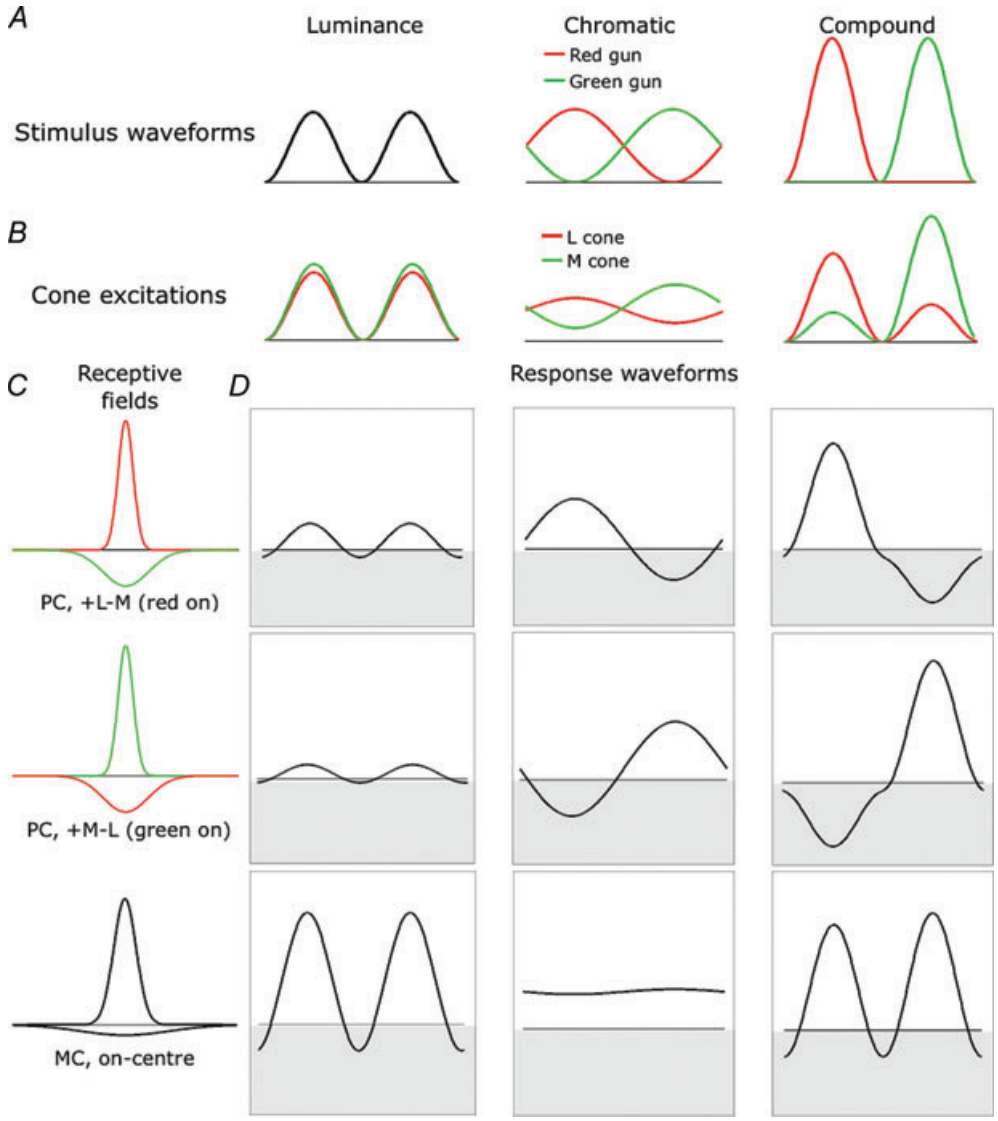

Figure 2. Prediction of model responses
A, stimulus waveforms for luminance, chromatic (red–green) and compound red–green gratings. The coloured curves refer to modulation of the red and green CRT guns at 100% contrast. All stimuli have the same mean luminance and chromaticity. *B*, cone excitations evoked by the different gratings calculated using the cone fundamentals and then normalized to mean chromaticity. *C*, receptive field profiles (difference-of-Gaussians model) for two PC cells (+L–M red on-centre, +M–L green on-centre) and an MC on-centre cell. Receptive field parameters were derived from the literature. *D*, responses of the three model cells to each grating type. Responses of PC cell models are weaker to luminance than to chromatic gratings, and are most vigorous to compound gratings, with some higher harmonic distortions. Responses of MC cell models are similar for compound and luminance gratings with little response to the chromatic grating. For recorded cells, some rectification of responses would be expected since firing rates cannot be negative, and this has been simulated by superimposing the responses on a maintained level (horizontal line); the shaded area indicates response structure which will be lost through rectification.

The model analysis predicts that compound gratings should evoke distinctive responses from PC and MC cells: PC cells should give similar responses to compound and chromatic gratings (especially after rectification), and MC cells similar responses to compound and luminance gratings. In the first part of this paper we test the accuracy of the model prediction; we then compare psychophysical detection and discrimination thresholds, to infer contribution of signals from the PC and MC pathways' tuning curves.

Physiological results

PC and MC cell responses to compound gratings. In this section we describe cell responses to chromatic, compound and luminance gratings. We recorded responses of 20 PC and 21 MC cells to luminance, chromatic and compound gratings over a range of spatial and temporal frequencies and contrasts.

Figure 3 shows responses of two typical PC cells (*B*, +L–M cell: *C*, +M–L cell). Responses are shown to a

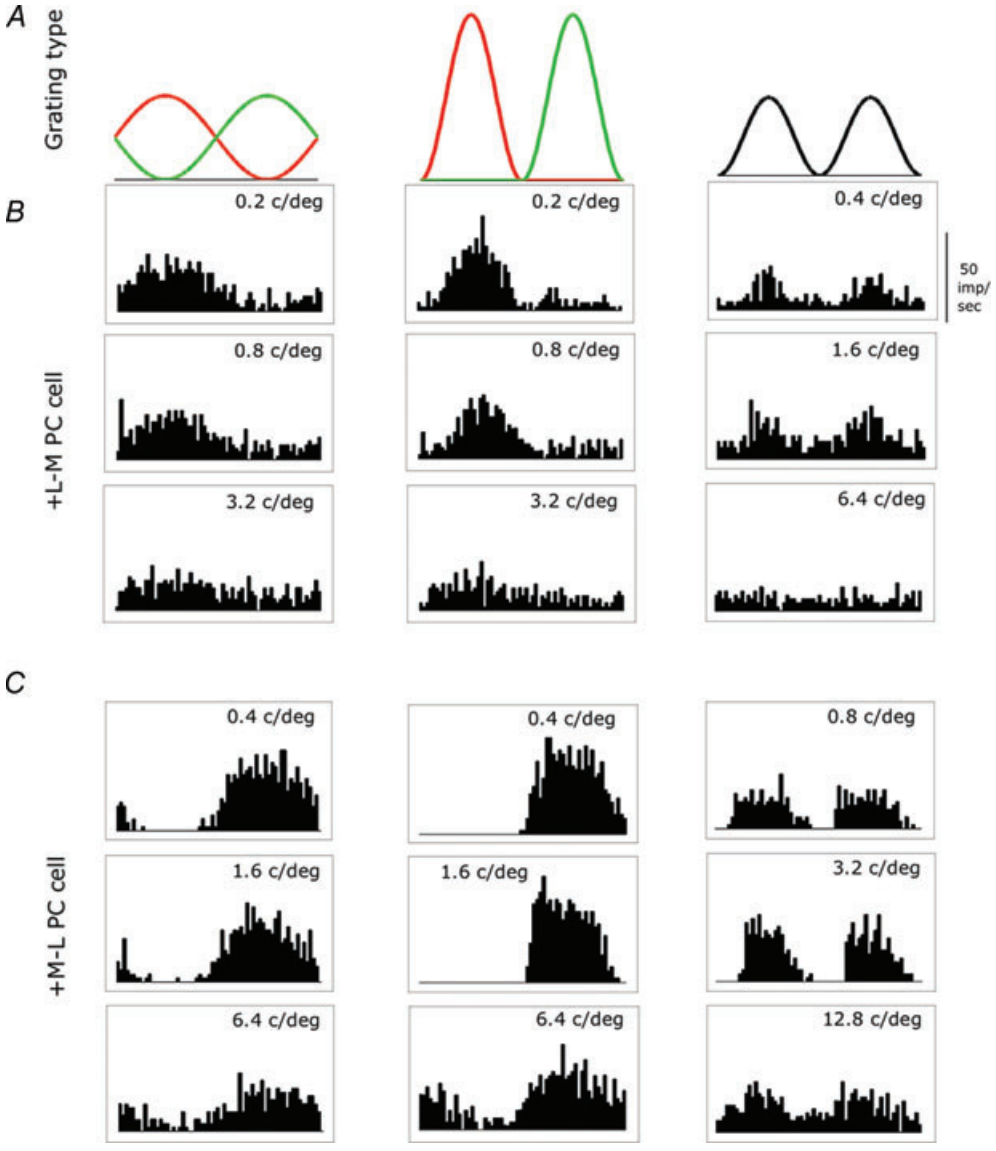

Figure 3. Responses of +L–M and +M–L cells to the chromatic red–green, compound red–green, and luminance gratings
A, grating waveforms. The gratings drifted at 1.6 Hz (3.2 Hz for luminance grating) and 75% of maximal contrast. Responses are averaged over 30 cycles. *B* and *C*, responses of +L–M and +M–L cell, respectively, at three spatial frequencies. The response to the compound grating is similar to, but larger than, the response to the chromatic grating. There is no obvious second-harmonic response to the compound grating, even at the highest spatial frequency.

drifting grating at 75% of maximal modulation contrast at spatial frequencies as indicated; three out of the eight frequencies tested are shown. The luminance grating has twice the spatial and temporal frequency of the chromatic and compound gratings, in order to match the luminance component of the compound grating. Response amplitude decreased with spatial frequency for the chromatic and compound gratings. PC cell responses to compound and chromatic gratings were similar, as expected from the model results in Fig. 2, and there was no indication of a second-harmonic response (dual peaks) to the luminance component in the compound grating at any spatial frequency; responses to the compound grating were generally larger than to the chromatic grating, and tended to have more sharply defined peaks. This is largely due to the higher chromatic contrast of the former (see Appendix). Off-centre cells showed similar results, with some response waveform differences.

Figure 4*A* shows Fourier spectra for the cells in Fig. 3 for each grating variety (0.8 cpd for chromatic and compound, 1.6 cpd for luminance gratings). The 1st harmonic response amplitude to the compound grating was greater than to the chromatic grating, and there was more energy in the higher harmonics. A larger response to the compound grating is expected since root-mean-square chromatic contrast (see eqn (4) in Appendix) is greater for the compound grating.

The 'double-duty' hypothesis (e.g. Ingling & Martinez-Uriegas, 1985) suggests that both chromatic or luminance information might be multiplexed within signals carried by PC cells, with the luminance component dominant at higher spatial frequencies. If this were so, it might be expected that at high spatial frequencies there should be two response peaks per stimulus cycle for the compound gratings at high spatial frequencies. This was not apparent (Fig. 3). Figure 4*B* shows tuning curves for the two cells. For compound and chromatic gratings, 1st harmonic (1F) tuning curves are low pass, and for luminance gratings a band-pass character is apparent, as expected. However, the 2nd harmonic

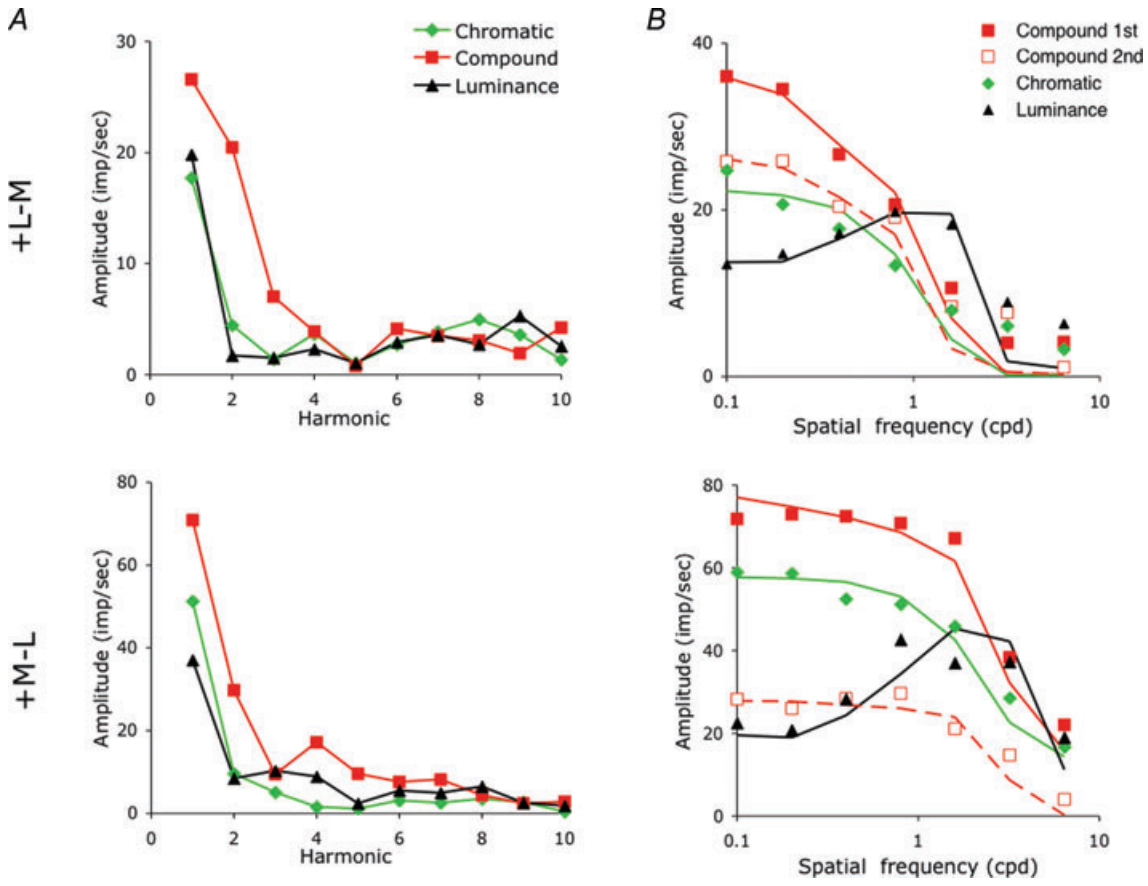

Figure 4. Harmonic composition of PC cell responses
A, Fourier spectra of responses from Fig. 3 for the two cells shown (+L–M: 0.8 cpd; +M–L 1.6 cpd). There is a larger response of PC cells to the compound compared to the chromatic grating, expected from the higher chromatic contrast. *B*, spatial frequency tuning curves for the two cells for the different grating types. For the compound grating, the tuning curves for 1F and 2F response components are shown. For the luminance grating, the band-pass tuning is apparent, but this is not visible in the 2F response component. Curves represent fits of the model described in Fig. 2.

tuning curve for the compound grating is low pass and similar in shape to the 1F curve. This suggests that the 2F response reflects higher-harmonic distortion of the 1F response, i.e. the chromatic response to the compound grating is dominant at all spatial frequencies. The continuous curves associated with each set of points represent fits of the model sketched in Fig. 2. Rectified responses (as shown in Fig. 2) were Fourier analysed and response amplitudes fitted to the data with a least squares criterion using a grid search. Free parameters were centre and surround radii, centre/surround weighting, an amplitude scaling factor and the maintained activity level, which determines the degree of response rectification. The model provides a reasonable description of the data.

In most cells, the 2F response component to the compound grating did not show the band-pass character of the response to the luminance grating. This is attributable to the fact that, with balanced opponent mechanisms, the chromatic response is dominant, and higher harmonic components are associated with response rectification rather than the 2F luminance component of the compound grating. Only in 2 of 22 PC cells recorded was there a small indication of a 2F response to compound gratings at high spatial frequencies; in both these cells M/L cone balance was not close to one. These results suggest that luminance structure in compound chromatic patterns cannot be easily derived from PC cell activity.

MC cells are expected to respond to the luminance component of the compound grating, and this is illustrated in Fig. 5 for an on-centre and an off-centre MC cell; two spatial frequencies are shown. Responses were similar for the compound and luminance gratings. There was a small, frequency-doubled response to the chromatic grating (Lee *et al.* 1989*a*; Lee & Sun, 2009). Figure 6*A* shows Fourier spectra of the two MC cells of Fig. 5 at 0.2 cpd. For the compound grating, the energy in the response is in the even harmonics (connected points) and spectra resembled those for luminance gratings. There is a small 2F response to the chromatic grating.

Figure 6*B* shows the mean 2F/1F response ratio for the sample of PC and MC cells as a function of spatial

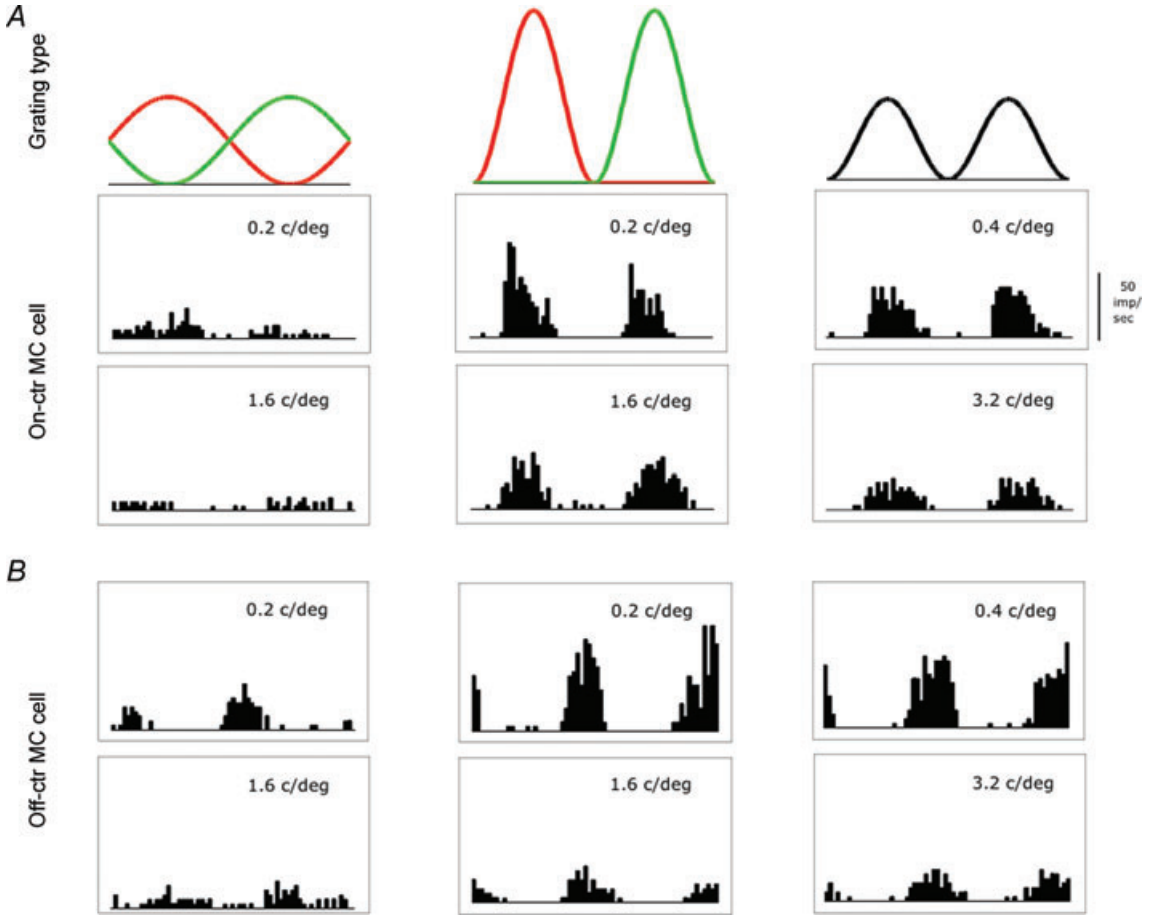

Figure 5. Responses of MC cells to chromatic, compound and luminance gratings
Stimulus parameters as in Fig. 3, except that only two spatial frequencies are shown. *A*, stimulus waveforms. *B* and *C*, responses of on- and off-centre cells, respectively. Responses to the compound and luminance gratings are very similar. There is a weak frequency-doubled response to the chromatic grating.

frequency for the compound and chromatic grating types. This is greatest for MC cells with compound gratings, indicating they transfer the luminance component of the pattern, which has twice the spatial frequency. For compound gratings and PC cells, the ratio remains below one, and is similar over all frequencies, consistent with the analysis in Fig. 4 that indicated that a switch from chromatic (which has a fundamental frequency) to luminance signalling (which has twice the spatial frequency) does not occur as a function of spatial frequency. For comparison, the ratio is also shown for PC cells and chromatic modulation, and for MC cells for chromatic stimuli, for which the high 2F/1F ratio is indicative of the frequency-doubled responses of MC cells to the chromatic grating.

The results in Figs 3–6 were for gratings of 75% of maximal modulation contrast. The psychophysical data shown in a later section were obtained at or near detection threshold. We explored the responses to the different gratings as a function of contrast to ascertain if the pattern of responses shown was independent of contrast. By eye, this appeared to be the case. To analyse this further, we plot in Fig. 7*A* the amplitude of 1F and 2F responses as a function of contrast for compound gratings near the optimal spatial frequency. Data shown were averaged from both +L–M and +M–L cells ($n = 10$, 5 of each). The 1F and 2F amplitudes increased in a parallel manner; their ratio is shown in Fig. 7*B* and, apart from the lowest contrast when responses were weak and the estimate noisy, it remained stable. In Figs 3–6, it was shown that the 2F response was not obviously associated with the luminance component of the compound grating. A further issue is variability, i.e. the reliability, of the 2F response. If variability were lower than that of the 1F response then, despite low amplitude, they might deliver a useful signal. To test this, the signal-to-noise ratio was calculated. There is a convenient estimate for noise in responses to sinusoidal modulation (Croner *et al.* 1993), defined as

$$\text{Noise} = \sqrt{\frac{\sum_1^n d_i^2}{n-1}} \quad (1)$$

where d_i is the distance in the complex plane between each individual response and the mean response. Noise was

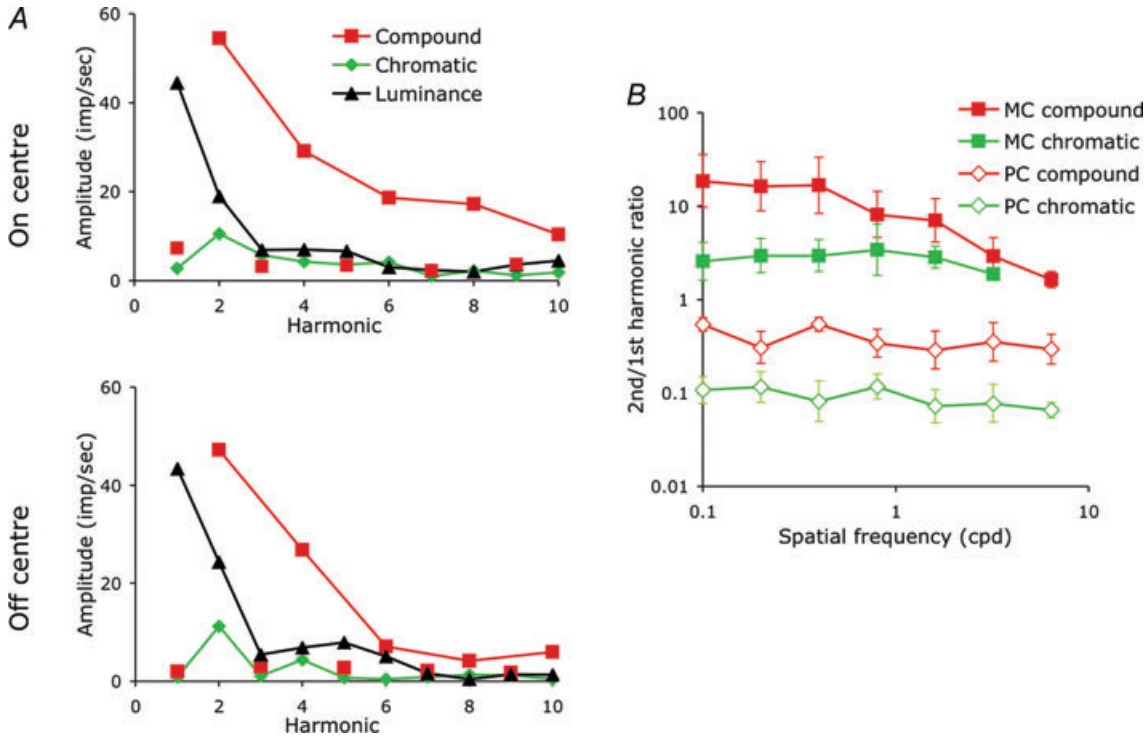

Figure 6. Fourier composition of MC cell responses
A, Fourier spectra of responses from Fig. 5 for the lower spatial frequency shown. For the compound grating, the response energy is largely in the even harmonics due to the luminance response, and just these values have been connected by line segments. Spectra for luminance and even harmonic compound responses are similar. There is a small 2F response to the chromatic grating. *B*, ratios of 2F to 1F harmonic amplitude under different conditions for different cell types as a function of spatial frequency. Data for PC cells were also shown as a comparison. Ratios are highest for MC cells and compound gratings as expected (averaged over 10 cells, on and off cells combined, only responses greater than 10 impulses s^{-1} included; 2 Hz, 75% of maximal contrast). Ratio remains similar over spatial frequency for PC cells for compound gratings (average of 10 cells, only responses greater than 10 impulses s^{-1} included; 2 Hz, 75% of maximal contrast).

calculated for the 1F and 2F responses. It is comparable for both (Fig. 7*A*) and independent of contrast (Croner *et al.* 1993; Sun *et al.* 2004). The signal-to-noise ratios for 1F and 2F responses are plotted in Fig. 7*B* and are a factor of 2–3 lower for the latter. This indicates that as contrast decreases, a significant 1F response persists to lower contrasts than does the 2F response; at low contrast the 2F signal becomes noisy. Figure 7*C* and *D* shows similar analyses for responses to chromatic gratings. Again the 2F amplitude increased parallel to the 1F response but was smaller than with the compound grating. These data suggest that 2F responses of PC cells to compound and chromatic gratings become less significant as contrast decreases. The ability of human observers to detect the difference between the gratings at detection threshold thus becomes of interest, and is discussed in a later section.

The PC cells' 1st harmonic response amplitude to the chromatic grating was consistently weaker than to the compound grating. We fitted curves for each cell with a Naka-Rushton function and calculated contrast gain (Naka & Rushton, 1966). This was 1.48 times larger for the compound than chromatic grating, a result that was highly significant (paired t test, $P < 0.01\%$). This value approximates the theoretical ratio of 1.71 between the chromatic contrast measures in eqn (4a,b) (see Appendix) for these gratings. This is relevant to differences in

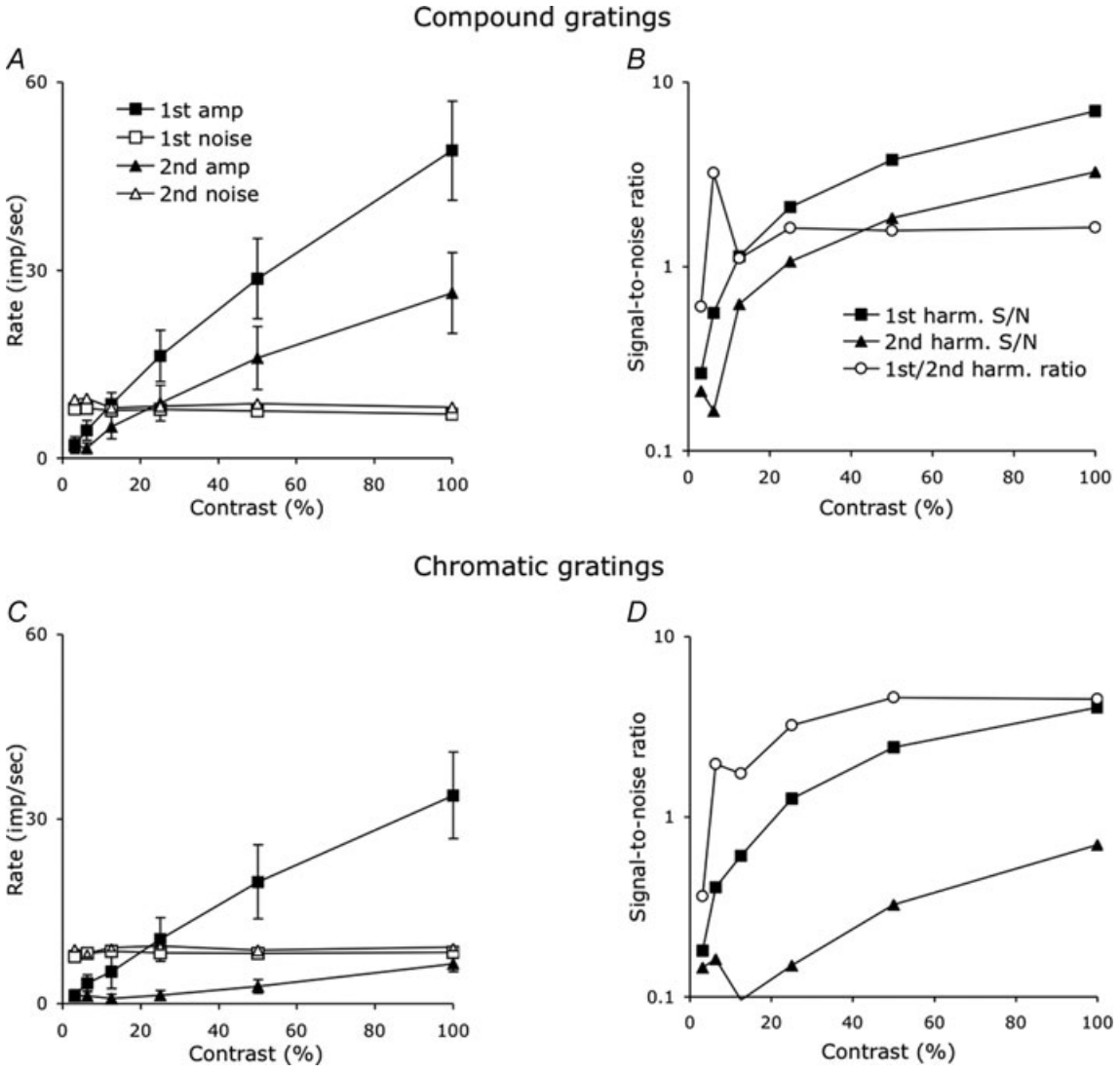

Figure 7. Responses of PC cells to compound and chromatic gratings as a function of contrast
A, amplitude of 1F and 2F components as a function of stimulus contrast together with estimates of response variability (i.e. noise). 1F responses are larger than 2F responses but noise is similar for both. Mean of 10 PC cells, +L–M and +M–L cells combined). Error bars are 95% confidence limits of the sample mean; most variability is due to inter-cell variation in response amplitude. *B*, the ratio 1F/2F is similar at all contrasts. Signal-to-noise ratio curves of 1F and 2F components are similar in form though differing in amplitude. *C* and *D*, similar analysis for responses to chromatic gratings.

observer sensitivity to chromatic and compound gratings, as discussed in the next section.

We also explored cell responses to the different gratings as a function of temporal frequency from 0.5 to 30 Hz. For PC cells, differences in the shape of response histograms between compound and chromatic gratings became less marked at higher frequencies because higher harmonic distortion increased with both types (not shown). Otherwise the results of the analyses in previous figures remained valid over the temporal frequency range tested. The temporal response of PC cells (Lee *et al.* 1990) was low pass, i.e. sustained, with compound gratings and resembled the chromatic temporal response (not shown). For MC cells, the temporal response to compound gratings was band pass, i.e. transient, and resembled their luminance temporal frequency tuning curve (Lee *et al.* 1990).

Responses of cells with S-cone input to compound gratings

We measured responses of seven ganglion cells with excitatory S-cone input using grating sets in which the chromatic component modulated along a tritan confusion line, i.e. only S-cone modulation occurred. Again, a range of spatial and temporal frequencies and contrasts were studied. Cells with S-cone input show little centre–surround organization (Type II; Wiesel & Hubel, 1966; Tailby *et al.* 2008). One might therefore expect similar responses to compound and chromatic gratings. An example of response histograms of a +S–ML cell with blue–yellow compound tritan, equiluminant tritan and luminance gratings is shown in Fig. 8*A*. We show response histograms to the three grating types at three spatial frequencies as indicated. The responses to the equiluminant tritan and compound tritan gratings were similar and the response to the luminance grating was weak. The Fourier spectra were similar for the equiluminant tritan and compound tritan gratings as expected (Fig. 8*B*).

Psychophysical detection and discrimination

The physiological results are consistent with luminance and chromatic components of compound gratings being selectively carried in different pathways. We briefly describe psychophysical performance with detection and discrimination of these gratings. Data from all four observers were very similar; we show data from one observer (H.S.) here for red–green gratings. Similar results were obtained with blue–yellow tritan gratings.

Figure 9*A* shows spatial contrast sensitivity functions for equiluminant red–green and luminance gratings. Sensitivity is expressed in terms of 100/(percentage gun contrast). The equiluminant red–green contrast sensitivity function shows a typical low-pass shape. The luminance contrast sensitivity functions are band pass with a peak near ~3 cpd and spatial resolution limit near ~22 cpd. Chromatic sensitivities were ~0.3–0.5 log units higher than luminance sensitivities at the lowest spatial frequency,

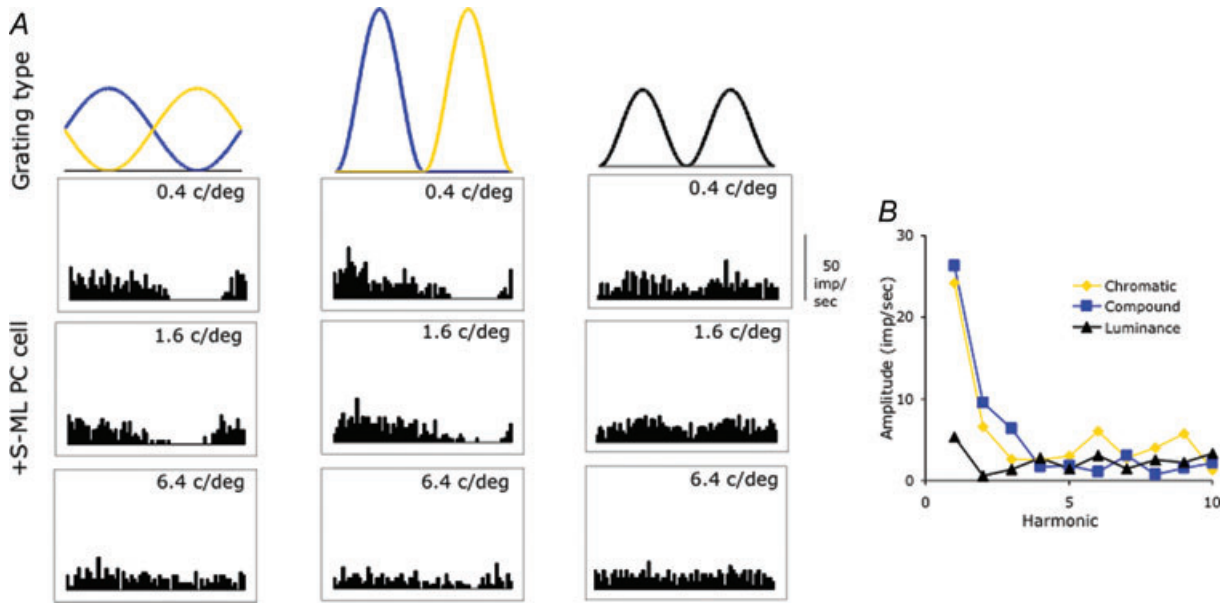

Figure 8. Responses of a blue-on cell to chromatic tritan, compound tritan and luminance gratings
A, responses plotted in a similar format to Fig. 3. Gratings drifted at 1.6 Hz (3.2 Hz for luminance grating) and 75% of maximal contrast. Responses are averaged over 30 cycles. The responses to the compound and chromatic gratings are very similar, and there is little response to the luminance grating. *B*, Fourier spectra of the responses. Responses of compound and chromatic gratings are similar; there is little response to the luminance grating.

and the two curves crossed at 0.3–0.6 cpd. For all observers, the equiluminant red–green sensitivity curves showed some irregularities at above ∼11 cpd, which was probably due to chromatic aberration effects. Apart from this, our data closely resemble those in the literature (e.g. Mullen (1985)).

If both luminance and chromatic signals carried in separate channels can contribute to detection of the compound grating, the spatial contrast sensitivity of the compound grating would follow the envelope of the luminance and chromatic contrast sensitivity functions. We plot spatial contrast sensitivity for red–green compound grating together with the fitted curves for the equiluminant and luminance gratings (dashed and continuous lines) in Fig. 9*B*. The luminance curves were shifted leftwards along the *x*-axis by a factor of 0.5 to match the luminance component in the compound grating. The chromatic curves were shifted up by a factor of 1.71 to

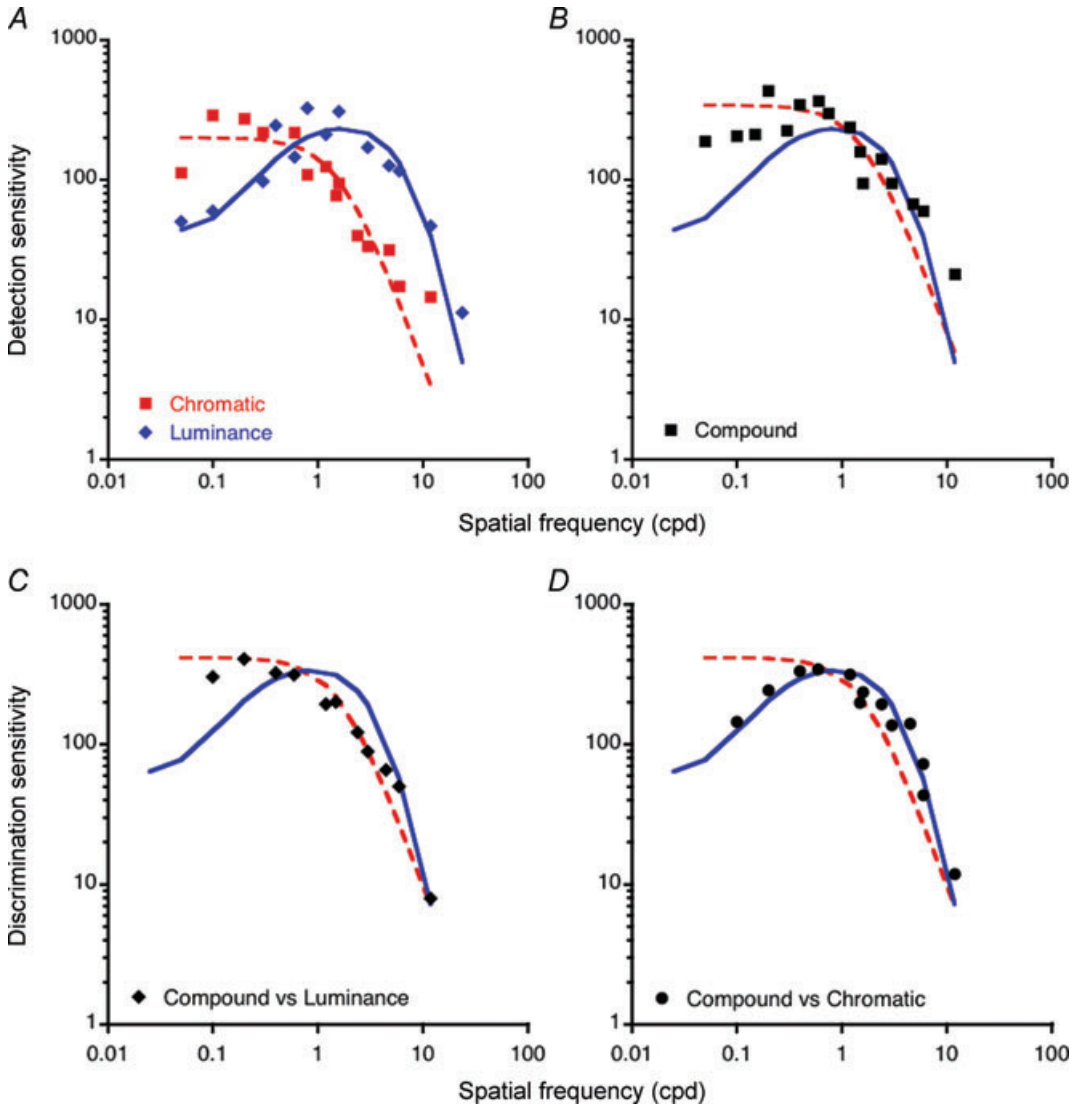

Figure 9. Psychophysical spatial contrast sensitivity functions of different grating types
A, detection thresholds for luminance and red–green chromatic gratings for one observer (H.S.). The curves represent filter fits for luminance and red–green chromatic contrast sensitivity functions. The chromatic contrast sensitivity function was fitted with a low-pass 2-stage filter (dashed line), and the luminance contrast sensitivity function was fitted with a band-pass filter which was the difference between a 3-stage and 1-stage low-pass filter. *B*, red–green compound grating detection thresholds with filter fits superimposed; the luminance fit was shifted leftwards along the *x*-axis by a factor of 0.5, and the chromatic curves were shifted up by a factor of 1.71 to take into account the greater chromatic contrast in the compound grating. *C* and *D*, discrimination sensitivity for red–green compound against red–green chromatic gratings, and compound against luminance gratings. These data are consistent with independent luminance and chromatic mechanisms underlying detection and discrimination.

take into account the greater chromatic contrast in the compound grating (see Appendix). Compound grating contrast sensitivity followed the envelope of the chromatic red–green and luminance contrast sensitivity curves.

These results are consistent with separable chromatic and luminance mechanisms contributing to the detection of the compound grating. If so, discrimination between compound and luminance, and between compound and chromatic gratings should be possible near threshold. On the other hand, if both chromatic and luminance information were carried in, say, the PC pathway, then the similarity of PC cell responses to chromatic and compound gratings and intrinsic noise (see above) would preclude discrimination near threshold. Fig. 9*C* and *D* shows discrimination thresholds for compound *versus* luminance gratings, and compound *versus* chromatic gratings. The chromatic and luminance sensitivity templates are also plotted. Discrimination between the compound and luminance gratings follows the chromatic sensitivity template. Discrimination thresholds between compound and chromatic gratings follow the luminance template. The results suggest that activation of both luminance and chromatic mechanisms are required to enable discrimination between the compound and chromatic gratings.

Psychophysical results for red–green compound gratings also held for blue–yellow compound gratings designed to isolate S-cone chromatic mechanisms (data not shown).

The results for both red–green compound gratings and blue–yellow compound gratings are consistent with compound gratings being detected and analysed by separable chromatic and luminance spatial channels; activation of both can contribute to detection and discrimination thresholds.

Discussion

We describe here a grating stimulus containing both luminance and chromatic components of different spatial frequencies. Combinations of luminance gratings of different spatial frequencies have been used in vision research, but grating combinations with luminance and chromatic components of different spatial frequencies have seldom been employed. The example shown here is just one member of a family of such combinations.

The results are consistent with physiological segregation of chromatic and luminance dimensions in different afferent pathways. Such segregation is thought to optimize information transmission from the retina in the presence of noise (Buchsbaum & Gottschalk, 1983; van der Twer & MacLeod, 2001). The results presented here indicate that straightforward segregation of luminance and chromatic information from PC pathway signals is difficult to achieve and argue against the multiplexing of luminance and red–green chromatic information within this pathway (Wiesel & Hubel, 1966; Ingling & Martinez-Uriegas, 1983; Lennie & D'Zmura, 1988). This does not mean to say that this pathway does not play a critical role in pattern vision; clearly the resolution of the mix of luminance and chromatic structure in Fig. 1 requires precise spatial information in both luminance and chromatic dimensions.

It should be stressed that luminance is defined by photometric tasks, and is likely to be based on the spectral sensitivity of MC cells (Lee *et al.* 1988; Kaiser *et al.* 1990; Valberg *et al.* 1992). The term 'achromatic channel' is sometimes used to refer to a mechanism underlying the perception of brightness or darkness dimensions of surfaces, which may be generated by a combination of PC cell activities (Valberg & Seim, 2008). These two mechanisms may be distinct, and may have distinct spatial properties, and distinct representations in the cortex; how such mechanisms relate to parietal and temporal cortical streams (Merigan & Maunsell, 1993) remains an open question.

To distinguish between the grating types, a comparison of MC and PC, or MC and S-cone cells is required at some central site. This points to a more nuanced view of combination of PC and MC signals in the cortex than just simple summation. For example, Kingdom (2003) demonstrated how interaction of luminance and chromatic signals generates a perception of depth. Combination of MC- and PC-pathway signals begin in area 17 (Johnson *et al.* 2004), but a detailed model by which central cells, or networks of cells, extract spatiochromatic information from visual patterns is lacking. Use of compound gratings as a stimulus may help identify MC and PC (and S-cone) inputs to cortical cells (Chen *et al.* 2007), and the way in which this information is further processed in the cortex.

Appendix

To generate a red–green compound grating on a CRT monitor, the following waveforms, W_R and W_G, are applied to the red and green guns, respectively,

$$W_R = \begin{cases} (1-C)R_{max}/4 - CR_{max}(\cos(2\theta+\pi)+1)/2 & \\ & 0 < \theta < \pi \\ (1-C)R_{max}/4 & \pi < \theta < 2\pi \end{cases} \quad (2a)$$

$$W_G = \begin{cases} (1-C)G_{max}/4 & 0 < \theta < \pi \\ (1-C)G_{max}/4 - CG_{max}(\cos(2\theta+\pi)+1)/2 & \\ & \pi < \theta < 2\pi \end{cases} \quad (2b)$$

where C is modulation contrast, and R_{max} and G_{max} are peak red and green gun luminances, which are set to be equal. These waveforms are sketched in Fig. 2*A*. Luminance or chromatic gratings of the same mean luminance and chromaticity are generated with sinusoidal modulation of the red (eqn (3a)) and green (eqn (3b)) guns either in-phase or out-of-phase of one another, as

$$W_R = R_{max}(1 + C\cos(\theta))/4 \quad (3a)$$

$$W_G = R_{max}(1 + C\cos(\theta + \theta_0))/4 \quad (3b)$$

where θ_0 is 0 for a luminance grating and π for a chromatic grating.

Luminance contrast in the compound grating can be calculated in the standard Michelson form $(L_{max} - L_{min})/(L_{max} + L_{min})$ since the luminance modulation is sinusoidal. The chromatic contrast cannot be calculated in this way (see Fig. 2), and we suggest the following metric, which is of a similar form to root-mean-square luminance contrast:

$$C_{chrom} = \sqrt{\frac{\int_0^{2\pi} (L - M)^2 \, d\theta}{2\pi}} \quad (4a)$$

where L and M are cone excitations normalized to the mean chromaticity. Using this measure, the chromatic contrast of the compound grating (0.612) is greater than that of the chromatic grating (0.354) by a factor of 1.71 (for 100% modulation contrast in eqn (2)). The same ratio is obtained if the contrast is calculated using red and green gun luminances, i.e.

$$C_{chrom} = \sqrt{\frac{\int_0^{2\pi} (R - G)^2 \, d\theta}{2\pi}} \quad (4b)$$

where R and G are values of the red and green gun luminances after normalization so that $R_{max} = G_{max} = 1$.

References

Buchsbaum G & Gottschalk A (1983). Trichromacy, opponent colours coding and optimum colour information transmission in the retina. *Proc R Soc Lond B Biol Sci* **220**, 89–113.

Chen Y, Martinez-Conde S, Macknik S, Swadlow H, Alonso JM & Lee B (2007). Input to cells in macaque V1 revealed with a novel grating stimulus. *J Vis* **7**, 57.

Cole GR, Stromeyer CFS III & Kronauer RE (1990). Visual interactions with luminance and chromatic stimuli. *J Opt Soc Am A* **7**, 128–140.

Croner LJ & Kaplan E (1995). Receptive fields of P and M ganglion cells across the primate retina. *Vision Res* **35**, 7–24.

Croner LJ, Purpura K & Kaplan E (1993). Response variability in retinal ganglion cells of primates. *Proc Natl Acad Sci U S A* **90**, 8128–8130.

Crook JM, Lange-Malecki B, Lee BB & Valberg A (1988). Visual resolution of macaque retinal ganglion cells. *J Physiol* **396**, 205–224.

Derrington AM, Krauskopf J & Lennie P (1984). Chromatic mechanisms in lateral geniculate nucleus of macaque. *J Physiol* **357**, 241–265.

Derrington AM & Lennie P (1984). Spatial and temporal contrast sensitivities of neurones in lateral geniculate nucleus of macaque. *J Physiol* **357**, 219–240.

Drummond GB (2009). Reporting ethical matters in *The Journal of Physiology:* standards and advice. *J Physiol* **587**, 713–719.

Ingling CR Jr & Martinez-Uriegas E (1985). The spatiotemporal properties of the r-g X-cell channel. *Vision Res* **25**, 33–38.

Ingling CR & Martinez-Uriegas E (1983). The spatio-chromatic signal of the r-g channel. In *Colour Vision; Physiology and Psychophysics*, ed. Mollon J & Sharpe LT. Academic Press, London.

Johnson EN, Hawken MJ & Shapley R (2004). Cone inputs in macaque primary visual cortex. *J Neurophysiol* **91**, 2501–2514.

Kaiser PK, Lee BB, Martin PR & Valberg A (1990). The physiological basis of the minimally distinct border demonstrated in the ganglion cells of the macaque retina. *J Physiol* **422**, 153–183.

Kelly DH & van Norren D (1977). Two-band model of heterochromatic flicker. *J Opt Soc Am* **67**, 1081–1091.

Kingdom FAA (2003). Color brings relief to human vision. *Nat Neurosci* **6**, 641–644.

Lee BB, Kremers J & Yeh T (1998). Receptive fields of primate ganglion cells studied with a novel technique. *Vis Neurosci* **15**, 161–175.

Lee BB, Martin PR & Valberg A (1988). The physiological basis of heterochromatic flicker photometry demonstrated in the ganglion cells of the macaque retina. *J Physiol* **404**, 323–347.

Lee BB, Martin PR & Valberg A (1989*a*). Nonlinear summation of M- and L-cone inputs to phasic retinal ganglion cells of the macaque. *J Neurosci* **9**, 1433–1442.

Lee BB, Martin PR & Valberg A (1989*b*). Sensitivity of macaque retinal ganglion cells to chromatic and luminance flicker. *J Physiol* **414**, 223–243.

Lee BB, Martin PR, Valberg A & Kremers J (1993*a*). Physiological mechanisms underlying psychophysical sensitivity to combined luminance and chromatic modulation. *J Opt Soc Am A* **10**, 1403–1412.

Lee BB, Pokorny J, Smith VC, Martin PR & Valberg A (1990). Luminance and chromatic modulation sensitivity of macaque ganglion cells and human observers. *J Opt Soc Am A* **7**, 2223–2236.

Lee BB & Sun H (2009). The chromatic input to cells of the magnocellular pathway of primates. *J Vis* **9**, 151–158.

Lee BB, Valberg A, Tigwell DA & Tryti J (1987). An account of responses of spectrally opponent neurons in macaque lateral geniculate nucleus to successive contrast. *Proc R Soc Lond B Biol Sci* **230**, 293–314.

Lee BB, Wehrhahn C, Westheimer G & Kremers J (1993*b*). Macaque ganglion cell responses to stimuli that elicit hyperacuity in man: Detection of small displacements. *J Neurosci* **13**, 1001–1009.

Lee BB, Wehrhahn C, Westheimer G & Kremers J (1995). The spatial precision of macaque ganglion cell responses in relation to Vernier acuity of human observers. *Vision Res* **35**, 2743–2758.

Lennie P & D'Zmura MD (1988). Mechanisms of color vision. *CRC Crit Rev Neurobiol* **3**, 333–400.

MacLeod DIA & Van Der Twer T (2003). The pleistochrome: optimal opponent codes for natural colours. In *Color Perception: Mind and the Physical World*, ed. Mausfeld R & Heyer D. Oxford University Press, Oxford.

Merigan WH & Maunsell JHR (1993). How parallel are the primate visual pathways? *Ann Rev Neurosci* **16**, 369–402.

Mullen KT (1985). The contrast sensitivity of human colour vision to red–green and blue–yellow chromatic gratings. *J Physiol* **359**, 381.

Naka KI & Rushton WA (1966). S-potentials from colour units in the retina of fish (*Cyprinidae*). *J Physiol* **185**, 536–555.

Parry NRA, Kremers J, Murray I, McKeefry D & Lee BB (2010). Determination of chromatic and achromatic temporal frequency responses in the human electroretinogram using a temporal compound stimulus. *J Vis* **9**, 72a.

Pokorny J, Graham CH & Lanson RN (1968). Effect of wavelength on foveal grating acuity. *J Opt Soc Am* **58**, 1410–1414.

Rüttiger L & Lee BB (2000). Chromatic and luminance contributions to a hyperacuity task. *Vision Res* **40**, 817–832.

Rüttiger L, Lee BB & Sun H (2002). Transient cells can be neurometrically sustained; the positional accuracy of retinal signals to moving targets. *J Vis* **2**, 232–242.

Shapiro AG, Pokorny J & Smith VC (1996). Cone-rod receptor spaces with illustrations that use CRT phosphor and light-emitting-diode spectra. *J Opt Soc Am A* **13**, 2319–2328.

Smith VC, Lee BB, Pokorny J, Martin PR & Valberg A (1992). Responses of macaque ganglion cells to the relative phase of heterochromatically modulated lights. *J Physiol* **458**, 191–221.

Smith VC & Pokorny J (1975). Spectral sensitivity of the foveal cone photopigments between 400 and 500 nm. *Vision Res* **15**, 161–171.

Smith VC, Pokorny J, Davis M & Yeh T (1995). Mechanisms subserving temporal modulation sensitivity in silent-cone substitution. *J Opt Soc Am A* **12**, 241–249.

Stromeyer CF, Cole GR & Kronauer RE (1987). Chromatic suppression of cone inputs to the luminance flicker mechanism. *Vision Res* **27**, 1113–1137.

Sun H, Lee BB & Rüttiger L (2003). Coding of position of achromatic and chromatic edges by retinal ganglion cells. In *Normal and Defective Colour Vision*, ed. Mollon JD, Pokorny J & Knoblauch K, pp. 79–87. Oxford University Press, Oxford.

Sun H, Ruttiger L & Lee BB (2004). The spatiotemporal precision of ganglion cell signals: a comparison of physiological and psychophysical performance with moving gratings. *Vision Res* **44**, 19–33.

Tailby C, Szmajda BA, Buzas P, Lee BB & Martin PR (2008). Transmission of blue (S) cone signals through the primate lateral geniculate nucleus. *J Physiol* **586**, 5947–5967.

Valberg A, Lee BB, Kaiser PK & Kremers J (1992). Responses of macaque ganglion cells to movement of chromatic borders. *J Physiol* **458**, 579–602.

Valberg A & Seim T (2008). Neural mechanisms of chromatic and achromatic vision. *Color Res Appl* **33**, 433–443.

Van Der Twer T & MacLeod DI (2001). Optimal nonlinear codes for the perception of natural colors. *Network* **12**, 395–407.

Wiesel T & Hubel DH (1966). Spatial and chromatic interactions in the lateral geniculate body of the rhesus monkey. *J Neurophysiol* **29**, 1115–1156.

Author contributions

B.B.L. and H.S conceived and designed the experiments. The physiological experiments were performed at SUNY Optometry, New York (B.B.L., H.S.), and the psychophysical measurements at the Norwegian University of Science and Technology, Trondheim (H.S., A.V.). The physiological data were collected and analysed by B.B.L. and H.S, and the psychophysical data by H.S. and A.V. All three authors drafted and revised the article, and approved the final version of the manuscript.

Acknowledgements

This research was supported by National Institutes of Health Grant EY 13112 (B.B.L), and a Visiting Researcher Fellowship from the Norwegian University of Science and Technology, Institute of Physics to H.S.